AJDS LAZHAR Al-Azhar Journal of Dental Science
Vol. 28- No. 1- 71:80- January 2025
Print ISSN 1110-6751 | online ISSN 2682 - 3314
https://ajdsm.journals.ekb.eg
Oral Biology, Medicine & Surgical Sciences Issue *(Oral Biology, Oral Pathology, Oral Periodontology, Medicine, Oral & Maxillofacial Surgery)*

THERAPEUTIC EFFICACY OF TARGETED PACLITAXEL LOADED ON ALBUMIN NANOPARTICLES ON DMBA INDUCED ORAL SQUAMOUS CELL CARCINOMA

Abd El-Hamied Salah Eldin El-Zarka[1*], Amr Saad Abd Alwahab [2], Mohamed Mahmoud Ahmed [3]

ABSTRACT

Objective: This research was aimed to determine therapeutic efficacy of targeted paclitaxel loaded on albumin nanoparticles on DMBA induced oral squamous cell carcinoma (OSCC). **Subjects & methods:** The thirty Syrian male hamsters had been separated into three groups, each with 10 members, that had been all equal. GI: To serve as negative controls, animals were left untreated. For fourteen weeks, seven,twelve-dimethylbenz (a) anthracene was applied 3 times per week to right pouches of animals in groups GII and GIII. In GII: No additional therapy had been administered. Whilst animals in GIII had been injected intraperitoneally (IP) with nanoparticles ab blbumin bound (NAB) paclitaxel (PTX) (ten mg/kg) two times per week for 2 weeks. After termination of experiment, gross observations had been recorded. Then, animals had been euthanized, all pouches had been surgically excised, fixed, & processed for hematoxylin & eosin stain examination & immunohistochemical staining utilizing (BCL2) as anti-apoptotic marker. **Results:** In this research, outcomes discovered some variability across medicated G (GIII)contrasted toGII. IHC of BCL2 highly revealed variation among GI & GII as well as GII & GIII (p value < 0.001). **Conclusion:** Conjugation of folate on surface of NAB improved cellular uptake, infiltration, & blood brain barrier penetration. Folate modified NAB had been confirmed to be more efficient to induce apoptosis of OSSC with encapsulation of PTX.

KEYWORDS: HBP carcinoma, paclitaxel, albumin nanoparticles, apoptosis

INTRODUCTION

Oral cancer has been 1of most prevalent forms of cancer worldwide. Over ninety percent of oral cancer cases have been caused by oral squamous cell carcinoma, common malignant tumor of head & neck[(1)]. Valuable knowledge about carcinogenesis has been developed throughout experimental research on animal models. Accumulated evidences pointed out the successful results when utilizing 7,12-dimethylbenz (a) anthracene (DMBA) to rise tumor burden & to produce deeper invasion & more anaplastic cells for induced hamster buccal pouch (HBP) carcinoma[(2)].

1 of most popular & efficient antineoplastic chemotherapy drugs, paclitaxel, has been made naturally from bark of Pacific Yew (Taxus

1. Assistant Lecturer, Oral and Dental Pathology Department, Faculty of Dental Medicine (Boys- Cairo), Al-Azhar University, Egypt.
2. Assistant Professor, Oral and Dental Pathology Department, Faculty of Dental Medicine (Boys-Cairo), Al-Azhar University, Egypt.
3. Professor, Oral and Dental Pathology Department, Faculty of Dental Medicine (Boys-Cairo), Al-Azhar University, Egypt.

• ***Corresponding author*:** drabdoo88@gmail.com

DOI: *10.21608/ajdsm.2023.222776.1441*

brevifolia). It has broad spectrum of anticancer action, but is especially effective against non-small cell lung cancer, ovarian cancer, breast cancer, head & neck cancer, & Kaposi's sarcoma[3]. Mechanism of action of PTX has been to promote & stabilize microtubules & inhibit late G2or M phases of cell cycle which blocking cell cycle progression and mitosis, causing the cell death. For instance, apoptosis induction, which increases generation of early reactive oxygen species & hydrogen peroxide in cancer cells, has been the primary mechanism by which PTX produces its deadly impacts. PTX has been involved in controlling calcium signals & miRNA expression to promote cancer cell death & tumor treatment, according to other investigations[4]. While PTX has been frequently used in clinical settings, these issues must not be disregarded when looking for further chemotherapeutic choices. Due to PTX exceptionally poor water solubility, it has low bioavailability, volatile metabolism, high level of toxicity, & causes allergic reactions[5].

The nanotechnology -based chemotherapy has been focused on developing cancer diagnosis & therapy techniques, which promising treatment for cancer due to its low toxicity, high specificity, & excellent bioavailability[6]. nanocarriers have the potential to shield the anti-cancer compounds against biodegradation & allow targeted delivery to tumor cells by active tumor-targeting[7]. Researchers have been interested in albumin protein, one of common types of biomolecules utilized for targeted administration, because of its capacity for selective delivery, lack of toxicity, & lack of immunogenicity[8]. (NAB-PTX) is the first protein nanotechnology-based chemotherapeutic agent, this allowing a shorter infusion duration that can reduce the common toxic reactions of traditional PTX, and its special structure allows more PTX to enter the tumor tissue to play an anti-tumor effect[9].

It has potential to enable not just tumor localization but also targeted delivery of therapeutic drugs to malignant tissue, minimizing collateral hazardous side-effects. Folate receptors (FR) are overexpressed on cell surface in tumor-specific manner. Exploiting FR as diagnostic & therapeutic target has several distinctive benefits[10]. Folate-conjugated nanoparticles can be considered as promising low-toxicity and efficient active drug delivery systems for PTX [11].

It had been discovered that apoptosis, or programmed cell death, has been crucial for controlling OSCC, BCL-2family proteins control variety of signals for cellular life & death, which culminate at mitochondria where cell destiny has been ultimately determined, Because BCL-2 has been 1 of anti-apoptotic proteins, malignancies that overexpress BCL-2 must have worse prognosis since they have been predicted to act as oncogenes in cancer cells. Nevertheless, research examining importance of apoptotic proteins for OSCC prognosis has produced conflicting outcomes[12].

So, the primary aim of this research had been to define efficacy of NAB-PTX of DMBA induced HBP carcinoma. Evaluation depends on animal's general health examinations, HBP gross observations, histological tumor tissue differences and immunohistochemistry examinations using BCL2 as anti-apoptotic marker.

SUBJECTS AND METHODS

Chemicals

DMBA (0.5percent) had been gotten from Sigma-Aldrich company, solubilized in paraffin oil.

PTX (Bristol-Myers Squibb company, USA) was prepared by Dissolved in1% normal saline.

Animals

Thirty male Syrian hamsters, aged 5 weeks, weighing among Eighty &120g. Experimental hamsters had been housed in common boxes with bedding made of sawdust in controlled environment with humidity levels of thirty to forty percent, temperature of twenty±two ˚C, & light cycles of

twelve hours of light & twelve hours of darkness. Hamster in good condition walked steadily & easily, had clear, bright eyes, healthy skin, & soft, lustrous coat free of parasites, cuts, dry patches, & swellings.

Ethical Approval

Ethical approval cleared by ethical committee of Faculty of Dental Medicine (Boys- Cairo), Al-Azhar University, Egypt (Ethical Code No. 411/1942).

Experimental design

Three groups (Gs) of ten animals each had been created at random from animals. Following week of adjustment. While animals in GI (negative control) had been left untreated, right pouches of animals in GII and GIII had been painted 3times per week for fourteen weeks with0.5 percent DMBA in liquid paraffin. Animals in GII (positive control) did not get further treatment after that, but those in GIII (NAB-PTX) did so following completion of14-week DMBA painting experiment[13], NAB-PTX will be administrated intraperitoneally (ten mg/kg) two times per week for 2 weeks [14], then they were euthanized after 3 weeks follow up.

General health examinations

During the experiment, variations in animal's general health had been observed. Hamsters had been modified if they displayed any of following symptoms of illness or disease: wheezing, hair loss, silence, corner, diarrhea, discharge from nose or eyes, moisture around tail, or crowding in sneezing[15].

Tumor volume measurement

Gross observations of HBP mucosa, including mucosal thickness, exudation, ulcers, & tumours, had been made after trial was completed. Right cheek pouch had been then opened; animals had been put to death, & Vernier caliper had been used to gauge each tumor's diameter. Tumor volume, where 3diameters (mm) of tumor have been D1, D2 & D3, had been calculated by formula, Vmm3 = (4/3) π [(D1/2) (D2/2) (D3/2)] [15].

Sample collection & preparation

The right cheek pouch was excised, fixed in ten percent neutral buffered formalin, routinely processed, & embedded in paraffin blocks to be examined histologically & IHC utilizing BCL2 as anti-apoptotic marker.

Histopathological examinations

Fourm thick tissue slices from paraffin blocks had been cut using rotary microtome, processed, mounted on glass slides, & stained with hematoxylin & eosin for light microscopic examination.

Measurement of depth of invasion

H&E stain slides were used to calculate DOI of each surgical specimen. From basal layer of surface epithelium to deepest site of tumor infiltration, DOI had been estimated. American Joint Committee on Cancer further divides it into three categories: less invasive at ≤five mm, moderately invasive at six-ten mm, & extremely invasive at ≥ten mm[16] **(Fig.1)**. Leica QWIN V3image analyzer computer system (Switzerland), which had been run using Leica QWIN V3software, calculated DOI.

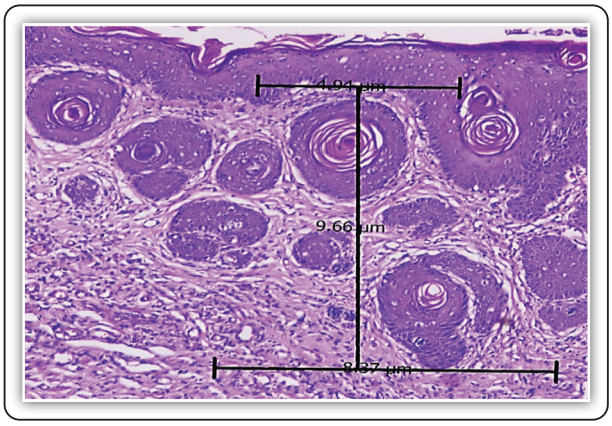

FIG (1) Photograph of measuring the DOI, by laying "plumb line" from horizon to deepest invasive nest, maximum invasion had been determined.

Immunohistochemical examination [17]

To demonstrate expression of BCL2antibody, additional tissue sections had been cut at four μm thickness & placed on positively charged slides for standard labelled streptavidin-biotin technique.

Positive control: To specify the bcl2 antibody as data sheet recommended, tissue sections of tonsillar tissue were stained and examined. Tissue sections revealed positive cytoplasmic brown staining**.**

Negative control: Process of staining continues after skipping primary antibody stage. To determine frequency of positive instances & localization of immunostaining within tissues, immunostained slices had been examined under light microscope. Additionally, image analysis computer system had been employed to determine area percent of immunostaining-positive cells.

Statistical analysis

After statistical analysis of gathered data, mean & standard deviation had been defined. Using SPSS version17.0 for Windows, a 1-way analysis of variance (ANOVA) had been carried out. ANOVA had been used with quantitative data & parametric distribution, together with post hoc analysis using LSD test, to distinguish among more than 2 distinct groups. Following p-values had been used to determine significance: p0.05 for significant, p>0.05 for non-significant, & p< 0.001for extremely significant.

RESULTS

Gross observations

No noticeable changes, such as hair loss or skin ulcerations, were found during **GI** examination. There were no inflammatory or pathological indications in normally pale pink HBP, **(Fig. 2 A)**. All the hamsters in **GII** showed signs of weakness, noticeable hair loss, & para-oral skin ulcerations. Right HBP mucosa found multiple exophytic variable size nodules with roughened granular surface. There had been bleeding & ulcerated spots all around nodules. **(Fig. 2B)**. 10 animals in **GII** with 10 tumor-bearing animals had an average tumor volume of 773.99 mm3 **(Table 1).** In **GIII,** all hamsters showed advancement in general health compared to animals in GII. In 6 hamsters out of 10, perioral skin ulcers & hair loss were seen as the end of GII, while the other 4 out of 10 had no perioral changes. Right HBP mucosa showed various variations, 5 hamsters out of ten found multiple exophytic small size nodules, surrounded with areas of ulceration & bleeding, while the other 5 hamsters found small exophytic nodules with lack of ulceration & bleeding **(Fig.2C)**. There was decrease in the mean tumor volume of GIII (435.11mm3) **(Table.1)** compared to that of GII.

Statistical analysis results of tumor volume:

Regarding **tumor volume**, there had been greatly variation (p value <0.001) among GII & (GIII). **(Table. 1 & Fig. 3).**

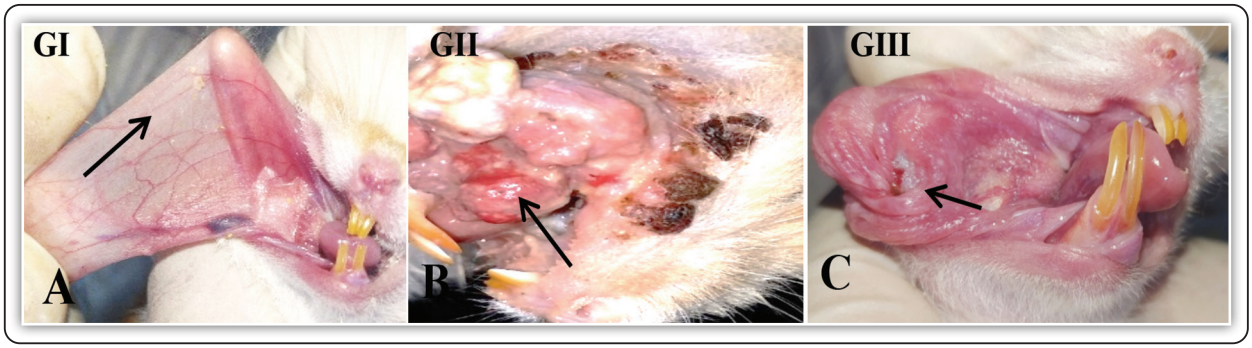

FIG (2) GI image displaying typical buccal pouch mucosa, which was pink in colour and had smooth surface (arrow). **(Fig.2B):** Exophytic papillary tumour masses with several foci of bleeding are visible in the GII image (arrow). **(Fig.2C):** Photograph of GIII indicating multiple exophytic nodules surrounded with area of necrosis (arrow).

TABLE (1) Comparing studied groups as regard to tumor volume.

	Tumor volume		P-value for post analysis usingLSD test	
	Mean ± SD	**Range**	**GII**	**GIII**
GII	773.99±56.27	693.2– 860.4	--	0.000
GIII	435.11±29.20	388.4– 473.1	0.000	--
F	**579.257**			
P-value	**<0.001 (HS)**			

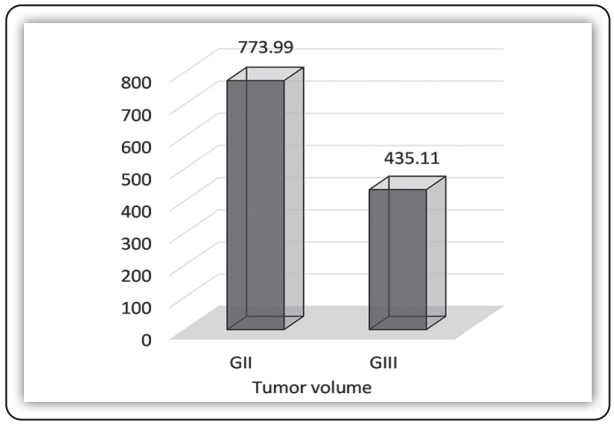

FIG (3) Comparing studied groups regarding tumor volume level.

Histological and IHC findings

Histological findings & IHC findings in tissue sections of HBP mucosa from experimental groups varied as follows:

GI: Using H&E stain on histological sections, it was discovered that normal thin stratified squamous epithelium has 2to 4layers of squamous cells that demonstrate light keratinization (i.e., 1layer of basal cells & 1, 2, or 3layers of spinous & thin keratinized cells without rete ridges). Sub epithelial CT, muscular layer & areolar layer had been seen **(Fig.4A)**. IHC staining utilizing **BCL2** antibody exhibited positive cytoplasmic expression (mean = 6.87%) **(Table.3)** which limited to basal & suprabasal epithelial layers **(Fig.4B).**

GII: Histological sections, using H&E stain, showed variable modifications. In seven hamsters out of ten exhibited well differentiated SCC and, other three hamsters exhibited moderate SCC. overlying epithelium showed multiple areas with dysplastic features consisting of pleomorphic, hyperchromatic nuclei exhibited altered nuclear/ cytoplasmic ratio and exhibited destruction of basement membrane. Well differentiated SCC with true invasion of malignant cells which appeared as epithelial pearls with keratin foci or cell nests or in form of detached & scattered cell with evidence of keratin formation. Moderately differentiated SCC was composed of cords or islands of neoplastic atypical epithelial cells, oval-shaped, round which infiltrated tumoral stroma with less keratin formation. **(Fig.4C).** The mean DOI revealed 9.68 mm **(Table.2)**. IHC staining using **BCL2** antibody exhibited positive cytoplasmic expression (mean= 70.83%) **(Table.3)** during epithelial layers & invading tumor cells **(Fig. 4D).** distribution ofBcl-2 immunoreactivity staining in OSCC cases showed most prominent expression in peripheral cells of infiltrating tumor islands which diminished toward center of the island in well-differentiated OSCC.

GIII: Histological sections, using H&E stain, discovered variable variations**:** In4 hamsters out of ten showed deeply invasive well differentiated SCC like in GII. other6 hamsters had well-differentiated SCC that showed superficial invasion of the malignant cells to the underlying CT and had not extended to the deeper parts, inflammatory infiltration was decreased, and the amount of keratin formation and collagen fibers were increased. There had been decrease of inflammatory reaction & rise amount of keratin formation and collagen fibers **(Fig.4E)**. The mean DOI in GIII (10 hamsters) was 2.24 mm **(Table.2)**. IHC staining using **bcl2** antibody exhibited positive cytoplasmic expression (mean= 48.51 %) **(Table.3)** during epithelial layers & invading tumor cells **(Fig. 4F).**

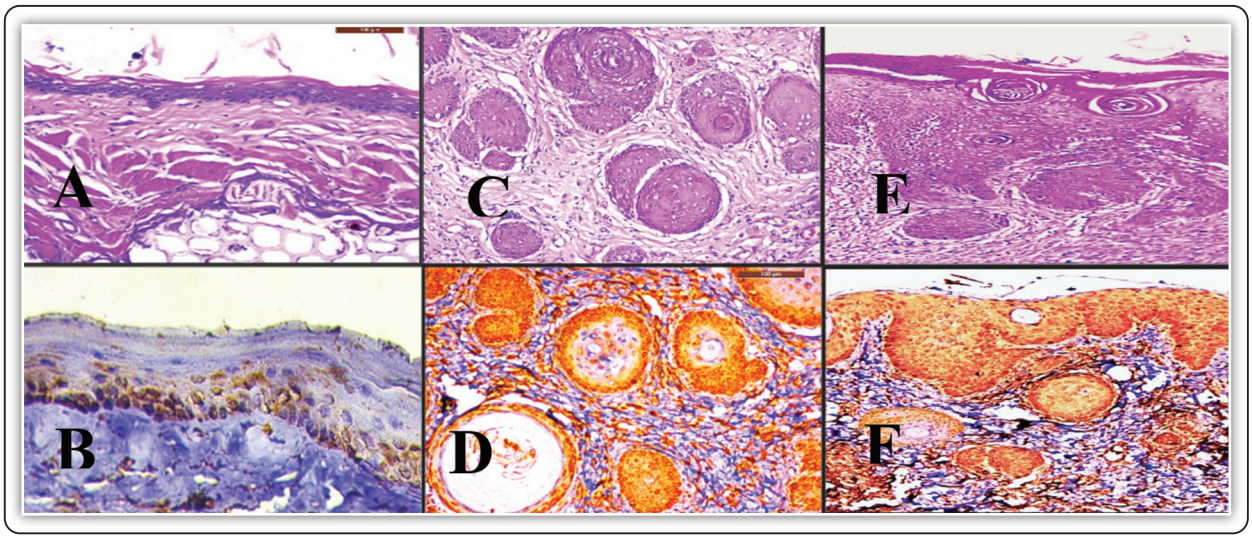

FIG (4) (A) Photomicrograph of GI indicating epithelium consists of2 to 4layers, superficial squamous cells exhibiting keratinization, flattened rete ridges, C.T layer, muscular layer, & deep layer of loose areolar connective tissue (H&E stain X100). (B) IHC staining using BCL2 antibody exhibited positive cytoplasmic expression limited to basal & suprabasal layers (Streptavidin biotin peroxidase, X 200). (C) Photomicrograph of GII revealing well differentiated SCC with deep invasion of multiple tumor islands into underlying connective tissue & sub-epithelial inflammatory infiltrates (H&E stain X200). (D) IHC staining using BCL2 antibody exhibited positive cytoplasmic expression during epithelial layers & invading tumor cells. (Streptavidin biotin peroxidase, X 200). (E) Photomicrograph of GIII indicating well differentiated SCC (superficial invasion) (H&E stain X100). (F) IHC staining using BCL2 antibody exhibited positive cytoplasmic expression during epithelial layers and invading tumor cells (Streptavidin biotin peroxidase, X 100).

Statistical analysis results of DOI

Regarding DOI, there had been greatly variation (p value < 0.001) among GII & the treated Gs (GIII). **(Table. 2 & Fig.5).**

TABLE (2) Comparing studied groups regarding DOI

	DOI		P-value for post analysis usingLSD test	
	Mean ± SD	**Range**	**GII**	**GIII**
GII	9.66 ± 1.79	8.4 – 13.9	--	0.000
GIII	2.24 ± 0.69	1.4 – 3.8	0.000	--
F	**175.607**			
P-value	**<0.001 (HS)**			

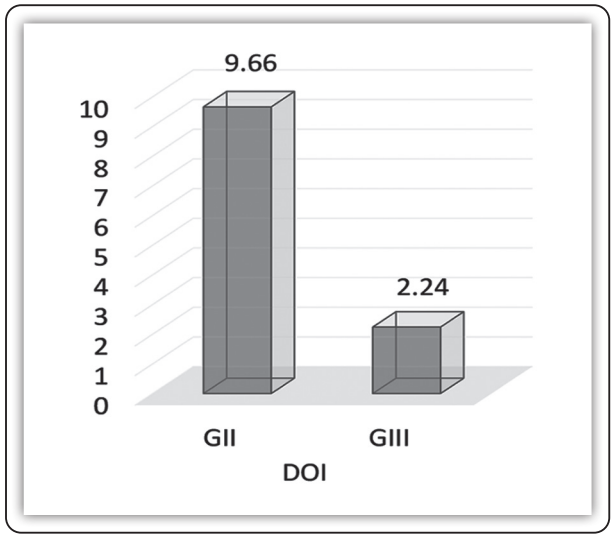

FIG (5) Comparing studied groups regarding DOI level.

Statistical analysis results of immune staining

Regarding BCL2, mean area % for GI was lowest (6.87%), while mean area % for GII was greatest (70.83%). variation among GI and GII had been highly significant (p value <0.001). When GII and GIII were compared, there had been highly variation among two (p value <0.001) **(Table. 3 & Fig. 6)**.

TABLE (3) Comparison among studied groups regarding BCL2 level.

	Bcl2		P-value for post analysis usingLSD test		
	Mean ± SD	**Range**	**G1**	**GII**	**GIII**
G1	6.87±1.50	4.2 – 9.1	--	0.000	0.000
GII	70.83 ±4.47	63.8 – 76.8	0.000	--	0.000
GIII	48.51±2.48	43.6 – 52.8	0.000	0.000	--
F	**497.581**				
P-value	**<0.001 (HS)**				

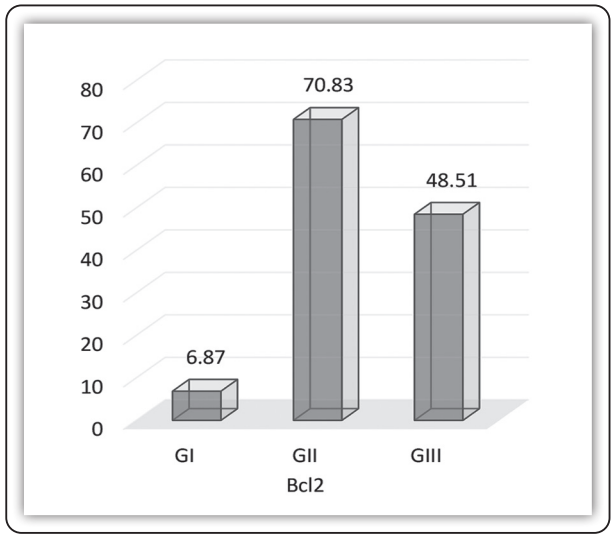

FIG (6) Comparing studied groups regarding BCL2 level.

DISCUSSION

To address whether value of nano Paclitaxel as targeted chemotherapeutic drug for treatment and inhibition of tumor progression of DMBA induced OSCC, this study was done. this was the first study to assess efficacy of paclitaxel loaded on albumin nanoparticles on DMBA induced HBP carcinoma. Outcomes of animal's general health examinations, HBP gross observations, H&E stain and IHC examination using BCL2, revealed variable observations.

OSCC has been most frequently diagnosed oral cancer To overcome the limitations of Chemotherapy, Numerous preclinical studies including nanoparticles based CDT delivery reported higher drug solubility, drug circulation times, & efficacy when compared to conventional free drug formulations are emerging in cancer therapy [18], even against chemo-resistant cell line. Impressive outcomes are obtained using nanoparticles to deliver[19].

In current research, gross observation results in **GI** didn't show any change, no perioral skin ulcerations, or hair loss. The HBP mucosa was found to be a normal pale pink color. These results agree with the studies reported the same findings [20]. After sacrificing, this result reflected on H&E staining which exposed normal thin stratified squamous epithelium formed of2 to 4cell layers, lacking rete ridges & thin keratin surface layer. These results agree with the studies reported by **Samah K et al.**, informed same result [21]. These results may be due to the hamsters not being exposed to the carcinogenic agent. IHC outcomes of Bcl-2in G1 found positive expression (mean = 6.7) **(table.3)**. only basal & suprabasal layers, respectively. This outcome could be attributed to bcl-2's role in regulating terminal differentiation of keratinocytes by shielding those cells' stem cells from apoptosis. Outcome of this research had been in agreement of some researches[22]. **Singh n et al.** [23] indicated that, under normal circumstances, Bcl-2ratio governs whether cell will survive or die through control of Cyt C's release from mitochondria.

In current research, gross observation results in **GII** exposed general debilitation of animals, perioral hair loss, and skin lesions, the HBP confirmed multiple exophytic variable size nodules surrounded by area of ulceration & bleeding. mean tumor volume of tumor-bearing animals had been 773.99mm^3 **(table.1)**. These findings have been mostly resulting of potent poisonous DMBA impact. This result agrees with another investigator[21].This result reflected on H&E staining in which DMBA-induced HBP tumors had been found numerous patterns of invasive OSCC (70% well differentiated & 30% moderately differentiated) in form of dysplastic lesions with deeper invading islands of epithelium into underlying connective tissues (DOI=9.66 mm) **(table.2)**. These results in consistence with that shown by other researchers[24]. These results can be referred to greater level of intracellular ROS throughout DMBA application which results in chronic oxidative stress[25]. Furthermore, all 3 phases of carcinogenesis—initiation, promotion, & progression—have been linked to ROS. Massive DNA damage brought on by the body's excessive ROS production has been linked to development of neoplasms. ROS-mediated DNA damage may alter DNA's structural properties, activate proto-oncogenes, & deactivate tumor suppressor genes, all of which can result in the development of cancer[26].

In current research, IHC staining of GII found positive cytoplasmic expression of BCL2 (70.85%) **(table.3)**. that was seen during epithelial layers & invading tumor cells, that showed greatly significantly expression compared to GI (p value <0.001). These outcomes have been in agreement with those of some studies[27, 28] Over expression of anti-apoptotic Bcl-2can contribute to that, Bcl-2prolong cell survival through inhibiting apoptosis by prevent release of Cyt C from mitochondria & can promote tumor development, similar results were observed by other investigators[29]. **Chen Yu *et al*** [28] also concluded that the cells located within infiltrating tumor nests were positively stained with BCL2 in OSCC cases.

In current work, GIII found relatively slight development in animal's general health compared to animals in GII. Right HBP mucosa showed a relative reduction in size of exophytic nodules. There was a decrease in the mean tumor volume (435.11mm3) with high significantly difference expression compared to that of GII **(table 1)**. These results conflicted on H&E staining in which4 out of 10 hamsters like GII, while the other 6 hamsters had well-differentiated SCC that indicated superficial invasion of malignant cells to underlying CT & had not extended to the deeper parts, and the amount of keratin formation and collagen fibers were increased. The mean DOI was (2.24 mm) that was decreased compared to GII with high significantly difference expression compared to GII (p-value = 0.001) **(table 2)**. These outcomes in consistence with that indicated by other researchers[30]. **Rajeshkumar et al** (2016)[31] Findings strongly suggested that NAB-PTX treatment had been superior to PTX treatment in stopping primary tumor growth, reducing the amount of thick tumor stroma, & consistently achieving stronger antitumor response. This improved the survival of tumor-bearing mice.

Furthermore, IHC expression of BCL2 in GIII revealed positive cytoplasmic expression (48.51) **(table.3)**. outcomes found high variation expression compared to GII (p-value = 0.001). In OSCC, This finding has been in agreement with that of other investigators[32]. expression levels of Bcl-2 had been dramatically reduced in tumors treated with Nab-PTX as compared with GII These results fit well with reduction in proliferation of tumor cells & considered to be the hallmark of apoptosis in mice treated with Nab-PTX in OSCC model. This outcome has been consistent with previous researchers' findings [33]. **L Lu et al (2019)** [34] showed that the folate NAB-PTX revealed the highest cytotoxicity to glioblastoma cells (LN229) & rise sensitivity of PTX to glioma cells that was assessed antitumor activity of drug-loaded nanoparticles by folate. Furthermore, conjugation of folate on surface of NAB improved cellular uptake, infiltration, & blood brain barrier penetration to be

more efficient to induce apoptosis of glioma cells with encapsulation of PTX. These results showed that BBB penetration & infiltration at tumor sites might be significantly increased by modifying folic acid on albumin nanoparticles. This outcome has been consistent with previous researchers' findings. [35] Gawde et al[35] concluded that addition of targeting ligand like folate has been important for formulation to be greatly efficient against cancer cells that over-express folate receptor. This demonstrates that formulation exhibits considerable impact through endocytosis or focused entry into cells mediated by folate receptor.

CONCLUSION

We have demonstrated that IP injection of folate modified NAB-PTX significantly boosts the antitumor efficacy of NAB-PTX This enhanced antitumor effect is likely due to fast extracellular NAB-PTX release in the tumor site and proved to be more effective to induce apoptosis of OSSC which improved cellular uptake, infiltration, & BBB penetration.

REFERENCES

1. Ezhilarasan D, Lakshmi T, Subha M, Deepak Nallasamy V, Raghunandhakumar SJOD. The ambiguous role of sirtuins in head and neck squamous cell carcinoma. 2022;28(3):559-67.
2. Farah CS, Shearston K, Nguyen AP, Kujan OJPcotoc. Oral carcinogenesis and malignant transformation. 2019:27-66.
3. Sharifi-Rad J, Quispe C, Patra JK, Singh YD, Panda MK, Das G, et al. Paclitaxel: application in modern oncology and nanomedicine-based cancer therapy. 2021;2021.
4. Ashrafizadeh M, Mirzaei S, Hashemi F, Zarrabi A, Zabolian A, Saleki H, et al. New insight towards development of paclitaxel and docetaxel resistance in cancer cells: EMT as a novel molecular mechanism and therapeutic possibilities. 2021;141:111824.
5. Feng T, Wei Y, Lee RJ, Zhao LJIjon. Liposomal curcumin and its application in cancer. 2017;12:6027.
6. Zhang Z, editor Feasibility of Nanotechnology in the Application of Cancer Therapy. E3S Web of Conferences; 2021: EDP Sciences.
7. Koning GA, Krijger GCJA-CAiMC. Targeted multifunctional lipid-based nanocarriers for image-guided drug delivery. 2007;7(4):425-40.
8. Shen X, Liu X, Li T, Chen Y, Chen Y, Wang P, et al. Recent advancements in serum albumin-based nanovehicles toward potential cancer diagnosis and therapy. 2021;9:746646.
9. Du X, Khan AR, Fu M, Ji J, Yu A, Zhai GJIjop. Current development in the formulations of non-injection administration of paclitaxel. 2018;542(1-2):242-52.
10. Wang J, Zhu M, Nie GJADDR. Biomembrane-based nanostructures for cancer targeting and therapy: From synthetic liposomes to natural biomembranes and membrane-vesicles. 2021;178:113974.
11. Rostami EJJoDDS, Technology. Progresses in targeted drug delivery systems using chitosan nanoparticles in cancer therapy: A mini-review. 2020;58:101813.
12. Bose P, Klimowicz AC, Kornaga E, Petrillo SK, Matthews TW, Chandarana S, et al. Bax expression measured by AQUAnalysis is an independent prognostic marker in oral squamous cell carcinoma. BMC cancer. 2012;12(1):332.
13. Saleh MM, Darwish ZE, El Nouaem MI, Mourad GM, Ramadan ORJADJ. Chemopreventive effect of green tea and curcumin in induced oral squamous cell carcinoma: An experimental study. 2020;45(3):74-80.
14. Hassan MS, Awasthi N, Li J, Williams F, Schwarz MA, Schwarz RE, et al. Superior therapeutic efficacy of nanoparticle albumin bound paclitaxel over cremophor-bound paclitaxel in experimental esophageal adenocarcinoma. 2018;11(2):426-35.
15. Al-Dosoki MA A-AA, Omar AMZ, Zouair MGA. Flow cytometric assessment of nivolumab and/or epigallocatechin-3-gallate on cancer stem cells of DMBA induced hamster buccal pouch carcinoma. Medical Science. 2021;25(118):3206-21.
16. Faisal M, Abu Bakar M, Sarwar A, Adeel M, Batool F, Malik KI, et al. Depth of invasion (DOI) as a predictor of cervical nodal metastasis and local recurrence in early stage squamous cell carcinoma of oral tongue (ESSCOT). PloS one. 2018;13(8):e0202632.
17. Kim S-W, Roh J, Park C-SJJop, medicine t. Immunohistochemistry for pathologists: protocols, pitfalls, and tips. 2016;50(6):411-8.
18. Marcazzan S, Varoni EM, Blanco E, Lodi G, Ferrari MJOo. Nanomedicine, an emerging therapeutic strategy for oral cancer therapy. 2018;76:1-7.

19. Chu S, Stochaj UJCDR. Exploring near-infrared absorbing nanocarriers to overcome cancer drug resistance. 2020;3(3):302.
20. Bruna F, Arango-Rodríguez M, Plaza A, Espinoza I, Conget PJScr. The administration of multipotent stromal cells at precancerous stage precludes tumor growth and epithelial dedifferentiation of oral squamous cell carcinoma. 2017;18:5-13.
21. El-Hossary WH, Hegazy E, El-Mansy MNJEDJ. Topical chemopreventive effect of thymoquinone versus thymoquinone loaded on gold nanoparticles on DMBA-induced hamster buccal pouch carcinogenesis (immunohistochemical study). 2018;64(4-October (Oral Medicine, X-Ray, Oral Biology & Oral Pathology)):3523-33.
22. A Al-Dosoki M, M Mansour A, M Ahmed MJA-AJoDS. Effect of oxygenated water as a new treatment modality on experimentally induced hamster buccal pouch carcinogenesis. 2018;21(3):261-73.
23. Singh R, Letai A, Sarosiek KJNrMcb. Regulation of apoptosis in health and disease: the balancing act of BCL-2 family proteins. 2019;20(3):175-93.
24. Sophia J, Kiran Kishore T K, Kowshik J, Mishra R, Nagini SJSr. Nimbolide, a neem limonoid inhibits Phosphatidyl Inositol-3 Kinase to activate Glycogen Synthase Kinase-3β in a hamster model of oral oncogenesis. 2016;6(1):1-13.
25. Suhail N, Bilal N, Hasan S, Ahmad A, Ashraf GM, Banu NJCS, et al. Chronic unpredictable stress (CUS) enhances the carcinogenic potential of 7, 12-dimethylbenz (a) anthracene (DMBA) and accelerates the onset of tumor development in Swiss albino mice. 2015;20:1023-36.
26. Arfin S, Jha NK, Jha SK, Kesari KK, Ruokolainen J, Roychoudhury S, et al. Oxidative stress in cancer cell metabolism. 2021;10(5):642.
27. Pallavi N, Nalabolu GRK, Hiremath SKSJJoO, JOMFP MP. Bcl-2 and c-Myc expression in oral dysplasia and oral squamous cell carcinoma: An immunohistochemical study to assess tumor progression. 2018;22(3):325.
28. Juneja S, Chaitanya NB, Agarwal MJIjoc. Immunohistochemical expression of Bcl-2 in oral epithelial dysplasia and oral squamous cell carcinoma. 2015;52(4):505-10.
29. Maheswari U. Expression of Annexin Al and KI-67 in histopathologically negative margins of oral squamous cell carcinoma cases with and without local recurrence: Vivekanandha Dental College for Women, Tiruchengode; 2018.
30. Bharadwaj R, Sahu BP, Haloi J, Laloo D, Barooah P, Keppen C, et al. Combinatorial therapeutic approach for treatment of oral squamous cell carcinoma. 2019;47(1):571-84.
31. Rajeshkumar N, Yabuuchi S, Pai SG, Tong Z, Hou S, Bateman S, et al. Superior therapeutic efficacy of nab-paclitaxel over cremophor-based paclitaxel in locally advanced and metastatic models of human pancreatic cancer. 2016; 115(4):442-53.
32. Riestra-Ayora J, Sánchez-Rodríguez C, Palao-Suay R, Yanes-Díaz J, Martín-Hita A, Aguilar MR, et al. Paclitaxel-loaded polymeric nanoparticles based on α-tocopheryl succinate for the treatment of head and neck squamous cell carcinoma: in vivo murine model. 2021;28(1):1376-88.
33. Ding J, Liu H-x, Xu W, Zhang X-l, Zhao R-x, Cheng X-y, et al. Nab-Paclitaxel is Far Superior to Traditional Paclitaxel. 2022.
34. Lu L, Shen X, Tao B, Lin C, Li K, Luo Z, et al. The nanoparticle-facilitated autophagy inhibition of cancer stem cells for improved chemotherapeutic effects on glioblastomas. 2019;7(12):2054-62.
35. Gawde KA, Sau S, Tatiparti K, Kashaw SK, Mehrmohammadi M, Azmi AS, et al. Paclitaxel and di-fluorinated curcumin loaded in albumin nanoparticles for targeted synergistic combination therapy of ovarian and cervical cancers. 2018;167:8-19.